Switching a Single Spin on Metal Surfaces by a STM Tip: *Ab Initio* Studies

Kun Tao,[1] V. S. Stepanyuk,[1,*] W. Hergert,[2] I. Rungger,[3] S. Sanvito,[3] and P. Bruno[1,4]

[1]*Max-Planck-Institute of Microstructure Physics, D-06120 Halle, Germany*

[2]*Fachbereich Physik, Martin-Luther-Universität, Halle-Wittenberg, Friedemann-Bach-Platz 6, D-06099 Halle, Germany*

[3]*School of Physics and CRANN, Trinity College, Dublin 2, Ireland*

[4]*European Synchrotron Radiation Facility, F-38043 Grenoble Cedex, France*

(Received 8 May 2009; published 30 July 2009)

The exchange coupling between single 3*d* magnetic adatoms (Cr, Mn, Fe, and Co) adsorbed on a Cu(001) surface and a Cr STM tip is studied with *ab initio* calculations. We demonstrate that the spin direction of single adatoms can be controlled by varying the tip-substrate distance, and the sign of the exchange energy is determined by the competition of the direct and the indirect interactions between the tip and the adatom. Based on the spin-dependent transport calculations, we find a magnetoresistance of about 70% at short tip-substrate distances.

DOI: 10.1103/PhysRevLett.103.057202 PACS numbers: 75.75.+a, 72.25.−b, 75.30.Et, 85.75.−d

The control over magnetic ordering down to a single atomic magnet, such as a single atomic spin on a surface, is of great importance for spintronics devices. The delicate interaction between the adatom and its surroundings, mediated by a supporting substrate or host, determines the resulting behavior of the spin orientation. The spin directions of interacting adatoms can be driven into either parallel (ferromagnetic) or antiparallel (antiferromagnetic) alignment, or even noncollinear alignment, depending on the sign of the exchange coupling. Recent scanning tunneling microscopy (STM) experiments demonstrate the ability to measure the exchange coupling between spins [1,2]. The magnetic exchange interaction can be obtained from the excitation spectra of a magnetic chain with different length [1] or the Kondo resonance of the interacting adatoms at various separations [2]. One can also use the magnetic exchange coupling to control the spin state of a single magnetic adatom by depositing it on an insulating thin film [3] or on magnetic islands [4,5]. Moreover, Heinrich *et al.* [6] have observed a spin-flip phenomenon for a single manganese adatom on a metal oxide island. In all the above experiments, the STM tip is only used as a tool probing the status of adatoms on surfaces, but the influence of the STM tip on electronic and magnetic properties of adatoms has not been investigated. However, theoretical and experimental studies have shown that electronic and magnetic properties, as well as the conductance behavior of a single adatom on metal surfaces, strongly depend on the tip-surface distance [7–12].

Here, we point out a way for manipulating the spin direction and the conductance of a single-atom-junction by a magnetic STM tip. We concentrate on the magnetic exchange coupling between single magnetic adatoms (Cr, Mn, Fe, Co) on a Cu(001) surface and a Cr tip. Performing *ab initio* calculations, we show that it is possible to control the spin direction of single adatoms with a magnetic STM tip by changing the tip-substrate distance. We demonstrate that the sign of the exchange coupling between the tip and the adatoms is determined by the competition of the direct and the indirect exchange interactions. A large magnetoresistance of about 70% is predicted for a single atom junction.

Our calculations are based on density functional theory (DFT). The ground state DFT calculations are performed using the VASP code [13] within the generalized gradient approximation (GGA), with the exchange-correlation functional of Perdew and Wang (PW91). The projector augmented wave (PAW) potentials are used [14] with a maximal kinetic-energy cutoff of 400 eV, and the total energy converges to 10^{-5} eV. The transport properties are calculated with the SMEAGOL code [15], which combines the nonequilibrium Green's function formalism with DFT [16]. For the SMEAGOL calculations, we use a standard double-ζ polarized basis for the Cu, whereas for Cr, we use a triple-ζ basis with 2 polarization orbitals for the *s* orbital. The cutoff radii of the first ζs are determined via an equivalent energy shift of 0.02 Ry, and higher ζs are constructed with the split-norm scheme [16]. A 2×2 in-plane *k*-point grid and a real space mesh cutoff of 350 Ry are used.

The Cu(001) substrate is modeled by a slab of 5 layers of Cu atoms with 16 atoms in each layer. The adatom is placed above the hollow site of the top Cu layer. We use a cluster model for the tip [17]. To simulate the STM tip, we use the following approaches: (1) the tip is modeled by a pyramid consisting of 13 Cu atoms and one Cr atom at the tip-apex (as shown in Fig. 1), and (2) by a pyramid consisting of 14 Cr atoms. In the latter case, since the Cr tip has an antiferromagnetic ground state [18], the spin direction of atoms in the second layer of the tip is set to be antiparallel to the spin direction of atoms in the other two layers. Three bottom Cu layers of the substrate and the top layer of the tip are fixed; all the other atoms are fully relaxed. The geometries are optimized until all residual forces on each atom are less than 0.01 eV/Å.

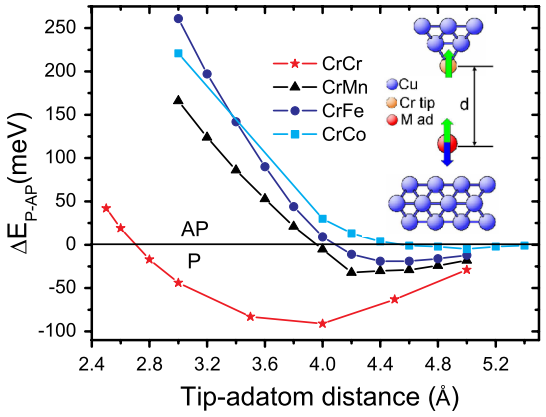

FIG. 1 (color online). Exchange energy as a function of the tip-adatom separation D. The inset is the setup for the calculations. In all calculations, the spin direction of the tip apex is fixed (spin up), while it can be reversed for adatoms (either to be spin up or spin down).

The magnetic interaction between the tip and adatoms can be inferred from the exchange energy E_{ex}, defined as $E_{ex}(D) = E_P(D) - E_{AP}(D)$, and displayed in Fig. 1, where E_P (E_{AP}) is the total energy of the system with the spin directions of the tip and the adatom in parallel (antiparallel) alignment, denoted as P (AP) configuration. For the interaction between the Cr tip and the Cr adatom, one can see that the exchange energy changes its sign when the tip approaches the surface. D_{Cross} is defined as the critical tip-adatom distance where the exchange energy changes its sign. A positive value of the exchange energy indicates that AP configuration is energetically favorable, while for negative values, the P configuration has the lowest energy. The exchange energy calculation without geometry relaxation has also been performed, and similar results were obtained. We have also carried out fully relaxed calculations for the exchange energies using the tip consisting of 14 Cr atoms. At the distance of 4.0 Å, the energy difference between P and AP configurations is about -77 meV, while it is 84 meV for 2.5 Å. Although exchange energies are quantitatively different from those of the single-Cr tip, the trends for both tip models are the same.

We have also studied the exchange interaction between the Cr tip and other magnetic adatoms, such as Mn, Fe, and Co (as shown in Fig. 1). Mn and Fe adatoms change their spin directions at the tip-adatom distance of about 3.8–4.0 and 4.0–4.2 Å, respectively, and it is about 4.6 Å for the Co adatom. In other words, going from the Cr to the Co adatom, the D_{Cross} increases. The above results give clear evidence that the magnetic exchange interaction between tip and adatoms can be controlled by varying the tip-adatom distance.

The transition from P to AP configuration can be traced by analyzing the charge distribution between the tip and the adatom. We concentrate on the charge distribution between the Cr tip and the Cr adatom at different tip-adatom separations in their ground states. The spin-dependent charge density difference $\Delta\rho^\sigma$ ($\sigma = \uparrow, \downarrow$) is defined as: $\Delta\rho^\sigma = \rho^\sigma_{CrCr} - \rho^\sigma_{CrCu} - \rho^\sigma_{tip}$, where ρ^σ_{CrCr} is the charge density of the Cr tip on Cr/Cu(001), ρ^σ_{CrCu} is that of the Cr adatom on Cu(001) surface, and ρ^σ_{tip} is for Cr tip. It is worth noting that the ρ^σ_{tip} and ρ^σ_{CrCu} are computed with the relaxed geometries as in the ρ^σ_{CrCr}. We present in Figs. 2(a) and 2(b) the charge density difference for majority (including s, p, and d orbitals) and minority (including s, p, and d orbitals) electrons at the tip-adatom separation of 4.0 Å (P configuration). It can be observed that there is a clear difference in the charge redistribution between the spin-up part and the spin-down part. For the spin-up part, an excess charge accumulates in the area between the tip apex and the adatom. It means that there is a charge transfer for the spin-up electrons from the tip and the adatom to the area between them. At the same time, for the spin-down electrons, there are only very few electrons depletion from the tip and the adatom, and the accumulation of the charge in the area between them is too weak to be visualized in the figure. Therefore, there is a spin-polarized charge transfer between the tip and the adatom, and this process includes mainly spin-up electrons.

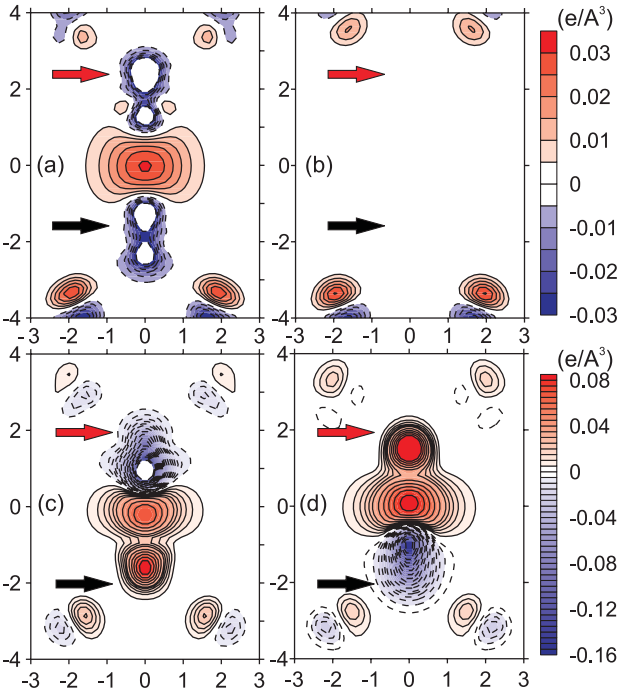

FIG. 2 (color). Spin-dependent charge density difference $\Delta\rho^\sigma$. The red and black arrows in the figure are the positions of the tip apex and the adatom, respectively. The units of the x and y axes are Å. (a) and (b) are the charge density difference for the spin-up and spin-down electrons at the tip-adatom separation of 4.0 Å (P configuration), respectively. (c) and (d) are the charge densities difference for the spin-up and spin-down electrons at the tip-adatom separation of 2.5 Å (AP configuration), respectively.

The spin-dependent charge density difference at the tip-adatom separation of 2.5 Å (AP configuration) is plotted in Figs. 2(c) and 2(d). One can find that the majority electrons deplete from the Cr tip apex and accumulate in the area between the tip and the Cr adatom. On the contrary, the Cr adatom loses the minority electrons while the tip receives them. In other words, there are two processes of the charge transfer, one is the transfer of the majority electrons from the Cr tip apex to the Cr adatom, and the second is the transport of the minority electrons from the adatom to the tip apex.

In order to make clear which orbitals are involved into the charge redistribution process, the projected density of states (PDOS) of the Cr adatom and the Cr tip apex at the tip-adatom separation of 4.0 Å (P configuration) is plotted in Fig. 3. The PDOS is obtained using SMEAGOL, so that the broadening of the peaks is induced by the coupling to the semi-infinite Cu leads. The PDOS generally agrees well with the one obtained using VASP. At a large tip-adatom separation, the direct overlap of the d states of Cr atoms is very weak. At the same time, a strong hybridization between the d and both the s and the p states can be observed for the tip apex and also for the adatom. The interaction between d states of the tip and d states of the Cr adatom occurs via the s- and p electrons. In other words, an indirect interaction between the tip and the adatom determines the exchange coupling between them. Our results can be explained with the classical Zener model [19,20]. The ferromagnetism of the incomplete d shells arises from the indirect coupling of the d shells via the conducting electrons (in this case, s and p electrons). All unpaired electrons within each atom strive to attain the configuration of the lowest energy, in which according to Hund's rule, all spins are parallel to each other. Since the conduction electrons carry along their own spins unchanged as they wander from atom to atom, they are able to move within an environment of parallel spins only if the spins of all the d shells are pointing in the same direction. This indirect coupling via the conduction electrons will therefore lower the energy of the system when the spins of the d shells are parallel. This is a so-called double exchange process. Ferromagnetism is possible only when the indirect coupling dominates over the direct coupling between adjacent d shells.

Now we can understand why the D_{Cross} for Cr, Mn, Fe, and Co adatoms are different. The coupling energy between the inner d electron and the outer s shell in atoms decreases from 0.92 eV for the Cr atom to 0.50 eV for the Co atom [21]. The reduced hybridization between s and d electrons promotes the transition from P to AP configuration. Therefore, going from Cr to Co the D_{Cross} increases. However, results for Mn, Fe, and Co are close.

At short tip-adatom separations, the scenario of the magnetic coupling in the junction is different. In this case, a direct interaction between d states of the tip and the adatom determines the ground magnetic state. Moriya pointed out that half-filled d shell couples with other atoms almost antiferromagnetically due to direct d-d covalent admixture [22]. Our results of the interaction between the half-filled Cr tip with magnetic adatoms at short tip-adatom distances can be well explained by Moriya's theory.

We now analyze how a change of the spin alignment between the tip and the adatom from the P to the AP configuration affects the current. The zero-bias transmission coefficients for the Cr tip and the Cr adatom at different tip-adatom distances D are presented in Fig. 4. The values for D go from 2.5 Å, where the AP configuration has the lower energy, to 4.0 Å, where the P configuration is the ground state, and where the ferromagnetic exchange energy is maximal (see Fig. 1). We first note that the transmission is of the order of 1 for energies around the Fermi energy, E_F. This indicates that for the chosen separations,

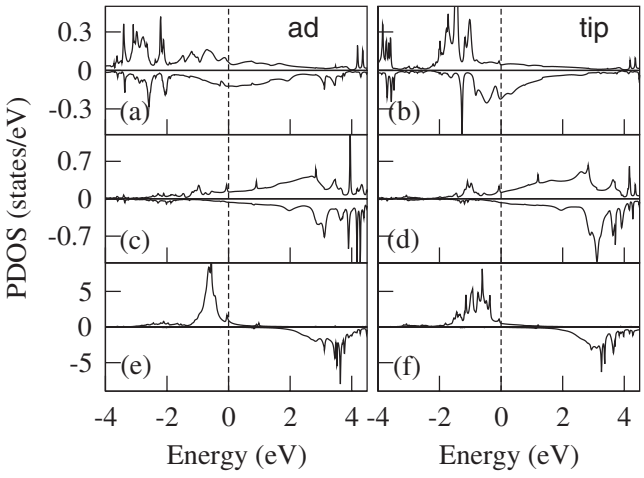

FIG. 3. Projected density of states for the Cr adatom (left panels) and the Cr tip- apex (right panels) at 4.0 Å separation between them (P configuration); (a), (b) 4s states; (c), (d) 4p states; (e), (f) 3d states.

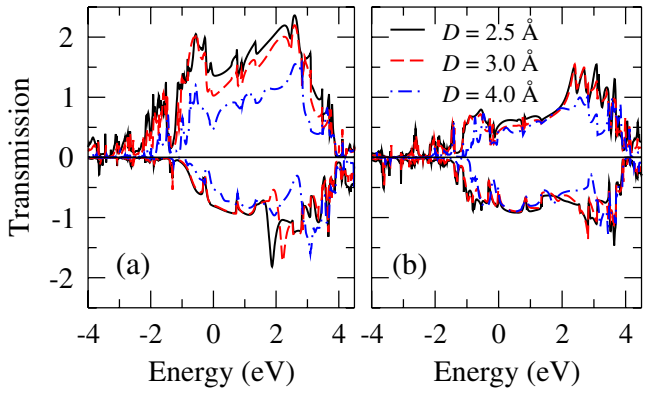

FIG. 4 (color online). Zero bias transmission coefficient for the Cr tip and the Cr adatom at different tip-adatom separations, D, for P (a) and AP alignment (b). Positive values are for majority spins, negative values for minority spins.

the electron transfer rate is large so that indeed a substantial interaction between tip and substrate can occur due to the conduction electrons. One can see that an increasing separation leads to a reduction of the transmission. Moreover, the width of the high transmission region is reduced, which is due to the decrease of the hopping between the tip and the adatom with increasing D. The transmission around E_F is in the range of 1 to 2, which shows that more than one channel significantly contributes to the total transmission. One can clearly attribute the various peaks in the transmission to peaks in the PDOS of Fig. 3. For $D = 2.5$ Å in the P configuration, the majority transmission is significantly larger than the one for the minority spins for energies up to E_F. This is due to the fact that whereas for the majority, there are significant contributions to the DOS from s, p, and d electrons, for the minority spins, the contributions from the p and d electrons are very small at these energies. The only available channel for the minority-spin electrons is therefore the s channel, and this results in a smaller transmission. For $D = 4$ Å, however, the difference in transmission between P and AP transmission is much smaller, which indicates that the extended $4s$ states give the main contribution to the transmission for large separations. For energies up to about 4 eV above E_F, the p orbitals also substantially contribute to the transmission. This analysis further supports our model of the double exchange coupling at large distances.

The AP transmission [Fig. 4(b)] can approximately be seen as a convolution of the majority and minority transmissions [15]. In this case, since the adatom and tip atom are both Cr atoms, it is approximately equal for majority and minority spins. For both spins, the AP transmission around E_F is smaller than the one of the P majority spins, but it is larger than the one of the P minority spins. The total transmission for the P configuration is, however, larger than the one for the AP configuration, the difference becoming larger with decreasing D. Therefore, a large magnetoresistance can be expected at small distances. The magnetoresistance ratio is defined as $R_{\mathrm{MR}} = (I_{\mathrm{P}} - I_{\mathrm{AP}})/I_{\mathrm{AP}}$, with $I_{\mathrm{P}}(I_{\mathrm{AP}})$ the current in the P (AP) configurations. At zero bias, R_{MR} can be obtained from the transmission at E_F, and we obtain $R_{\mathrm{MR}}(D = 2.5\ \text{Å}) = 73\%$, $R_{\mathrm{MR}}(D = 3.0\ \text{Å}) = 64\%$, and $R_{\mathrm{MR}}(D = 4.0\ \text{Å}) = 3\%$. We also calculate R_{MR} for the short tip-adatom separation of 2.5 Å by calculating the current for an applied bias of 0.2 V, for both the P and the AP configurations. Using the obtained currents, we find $R_{\mathrm{MR}} = 70\%$, in good agreement with the zero bias prediction. We note that the change of the resistance does not require external magnetic field.

In conclusion, our results have demonstrated that the spin direction of single magnetic adatoms can be controlled by varying the position of a spin-polarized STM tip. The physics behind all effects found in the present work is related to the competition of the direct and the indirect interactions between the tip and the adatom. Spin-dependent transport properties have been calculated, and a large magnetoresistance has been found at the separation where a switching of the magnetic adatom is predicted. The present work provides a theoretical prediction that is feasible with current technology to manipulate the spin direction of a single adatom, and to detect the switching by measuring the current at a constant voltage as function of the tip to substrate separation.

This work was supported by DFG (SPP1153, SPP1165). The Smeagol project (IR, SS) is sponsored by Science Foundation of Ireland. Part of the calculations were performed at the Irish Centre of High End Computing.

*stepanyu@mpi-halle.mpg.de

[1] C. F. Hirjibehedin *et al.*, Science **312**, 1021 (2006).
[2] P. Wahl *et al.*, Phys. Rev. Lett. **98**, 056601 (2007).
[3] C. F. Hirjibehedin *et al.*, Science **317**, 1199 (2007).
[4] Y. Yayon *et al.*, Phys. Rev. Lett. **99**, 067202 (2007).
[5] B. W. Heinrich *et al.*, Phys. Rev. B **79**, 113401 (2009).
[6] A. J. Heinrich *et al.*, Science **306**, 466 (2004).
[7] W. A. Hofer *et al.*, Rev. Mod. Phys. **75**, 1287 (2003).
[8] R. Z. Huang *et al.*, Phys. Rev. B **73**, 153404 (2006).
[9] N. Néel *et al.*, Phys. Rev. Lett. **98**, 016801 (2007).
[10] K. Tao *et al.*, Phys. Rev. B **78**, 014426 (2008).
[11] L. Vitali *et al.*, Phys. Rev. Lett. **101**, 216802 (2008).
[12] N. Néel *et al.*, Phys. Rev. Lett. **102**, 086805 (2009).
[13] G. Kresse and J. Hafner, Phys. Rev. B **48**, 13115 (1993); G. Kresse and J. Hafner, Phys. Rev. B **49**, 14251 (1994); G. Kresse and J. Furthmüller, Phys. Rev. B **54**, 11169 (1996).
[14] P. E. Blöchl, Phys. Rev. B **50**, 17953 (1994).
[15] A. R. Rocha *et al.*, Phys. Rev. B **73**, 085414 (2006); A. R. Rocha *et al.*, Nature Mater. **4**, 335 (2005); I. Rungger and S. Sanvito, Phys. Rev. B **78**, 035407 (2008).
[16] J. M. Soler *et al.*, J. Phys. Condens. Matter **14**, 2745 (2002).
[17] W. A. Hofer *et al.*, Phys. Rev. Lett. **87**, 236104 (2001).
[18] A. Kubetzka *et al.*, Phys. Rev. Lett. **88**, 057201 (2002).
[19] C. Zener, Phys. Rev. **81**, 440 (1951).
[20] C. Zener, Phys. Rev. **82**, 403 (1951).
[21] C. Zener and R. R. Heikes, Rev. Mod. Phys. **25**, 191 (1953).
[22] T. Moriya, Solid State Commun. **2**, 239 (1964).